Thermal Stability and Ablation Properties of Silicone Rubber Composites

Eung Soo Kim, Eun Jeong Kim, Jea Hun Shim, Jin-San Yoon

Department of Polymer Science and Engineering, Inha University, Yonghyun-dong, Nam-gu, Incheon 402-751, Korea

Received 27 December 2007; accepted 30 April 2008
DOI 10.1002/app.28633
Published online 14 July 2008 in Wiley InterScience (www.interscience.wiley.com).

ABSTRACT: Effects of incorporation of clay and carbon fiber (CF) into a high temperature vulcanized (HTV) silicone rubber, i.e., poly(dimethylsiloxane) (PDMS) containing vinyl groups, on its thermal stability and ablation properties were explored through thermogravimetric analyses (TGA) and oxy-acetylene torch tests. Natural clay, sodium montmorillonite (MMT), was modified with a silane compound bearing tetra sulfide (TS) groups to prepare $MMTS_4$: the TS groups may react with the vinyl groups of HTV and enhance the interfacial interaction between the clay and HTV. $MMTS_4$ layers were better dispersed than MMT layers in the respective composites with exfoliated/intercalated coexisting morphology. According to TGA results and to the insulation index, the HTV/$MMTS_4$ composite was more thermally stable than HTV/MMT. However, addition of CF to the composites lowered their thermal stability, because of the high thermal conductivity of CF. The time elapsed for the composite specimen, loaded with a constant weight, to break off after the oxy-acetylene flame bursts onto the surface of the specimen was employed as an index for an integrated assessment of the ablation properties, simultaneously taking into consideration the mechanical strength of the char and the rate of decomposition. The elapsed time increased in the order of: HTV < HTV/CF ≈ HTV/$MMTS_4$ < HTV/CF/$MMTS_4$ ≈ HTV/MMT < HTV/CF/MMT. This order was different from the increasing order of the thermal stability determined by TGA results and the insulation index. The decreased degree of crosslinking of the composites with $MMTS_4$ compared with that of the composite with MMT may be unfavorable for the formation of a mechanically strong char and could lead to early rupture of the HTV/$MMTS_4$ specimen. © 2008 Wiley Periodicals, Inc. J Appl Polym Sci 110: 1263–1270, 2008

Key words: thermal stability; ablation properties; silicone rubber; composites

INTRODUCTION

High performance rocket motors are critical for the development of short- or long-range missiles, various space vehicles, and small science-oriented rockets for aeroscopy and for experiments under minute gravity.[1,2] They are propelled by the thrust of the combustion gas produced by explosive burning of solid or liquid propellants. Because the temperature of the combustion chamber of rocket motors frequently exceeds 2000–4000 K,[3] thermal insulation materials are applied between the propellant and the motor case. The main purpose of the thermal insulation materials is to protect the rocket motor case against the hot combustion gas. The thermal insulation materials also have the following concomitant functions[4]:

1. Protection of propellant and deformation of motor case against external impacts.
2. Restriction of diffusive transfer of mobile substances from propellant and liner.
3. Reduction of the pressure drop induced at the junction points of the motor case.
4. Induction of combustion gas flow to the nozzle direction.

Ablative materials are more suitable for these purposes than high-temperature resistant materials. Thermal degradation of ablative materials and dissipation of the resulting volatile small molecules absorb some of the combustion heat.

Both thermochemical erosion and mechanical erosion take place because of the shearing flow of the combustion gas. The char produced from the thermal degradation should have sufficient mechanical strength to withstand the shearing of the combustion gas flow. The char layer reduces penetration of heat flux from the hot free stream.[5]

Styrene–butadiene rubbers, acrylonitrile–butadiene rubbers, ethylene–propylene–diene rubbers, and isobutene–isoprene rubbers are used as elastomeric thermal insulators. However, these rubbers can only be used for short-range rockets.

Because silicone rubber has higher thermal stability and flexibility together with superior gas permeability

Correspondence to: J.-S. Yoon (jsyoon@inha.ac.kr).
Contract grant sponsors: Defense Acquisition Program Administration, Agency for Defense Development.

© 2008 Wiley Periodicals, Inc.

TABLE I
Recipe for the Silicone Rubber Composites (Unit: wt %)

	LS-5	Carbon fiber	MMT	$MMTS_4$
HTV	1	–	–	–
HTV/CF	1	1	–	–
HTV/5 wt % MMT	1	–	5	–
HTV/5 wt % MMT S_4	1	–	–	5
HTV/CF/5 wt % MMT	1	1	5	–
HTV/CF/5 wt % MMT S_4	1	1	–	5

compared with other rubbers, some countries possessing advanced technologies have already applied silicone rubber as a thermal insulator for the ram jet combustion chamber.[6]

In this study, the thermal stability and ablation properties of silicone rubber and silicone rubber composites with clay and carbon fiber (CF) are explored via thermogravimetric analyses (TGA) and oxy-acetylene torch tests. Rate of weight loss and the insulation index are used to assess the ablation performance of the silicone rubber composites. A new method is proposed for an integrated evaluation of the ablative properties, taking into consideration the rate of thermal degradation as well as the mechanical strength of the char formed during the oxy-acetylene torch test.

EXPERIMENTAL

Materials

GP-30® (HTV) (Dow Corning Co.; dimethyl, methylvinylsiloxane dimethylvinyl terminated (>60%), dimethylsiloxane, dimethylvinyl terminated (30–60%), amorphous silica (10–30%), molecular weight of ~ 200,000) is poly(dimethylsiloxane) (PDMS) endblocked with vinyl groups containing vinyl-methylsiloxane units in the main chains.

HTV was cured with DMBPH(2,5-dimethyl-2,5-di(*t*-butylperoxy)hexane) (LS-5, Dow Corning). Cloisite®Na^+ (MMT) having 92.6 meq/100 g cation exchange capacity (CEC) was supplied by Southern Clay (Gonzales, TX). CF was obtained from Wooshin Chemtech (Korea) and was cut into samples with 5–6 mm in length. Bis(3-triethoxysilylpropyl)tetra sulfide silane (TEPTS) was purchased from Aldrich (St. Louis, MO).

Clay modification

After TEPTS (7 g) was hydrolyzed in a solution of methanol (65 wt %) and deionized water (35 wt %) added with hydrochloric acid for 10 min, clay (70 g) was introduced to the mixture and stirred at 70°C for 14 h. The residue after filtering was washed several times with methanol at room temperature and then dried in a vacuum oven at 60°C for 48 h. The modified clay ($MMTS_4$) was powdered to a size of 50 μ by using a blender.

Preparation of the composites

HTV/clay, HTV/CF/clay, and HTV/CF composites were prepared by the solution cast method. HTV was completely dissolved in toluene with 1 wt % of DMBPH. The resulting solution was stirred with clays under sonication for 3 h, and then dried in a vacuum oven at 60°C for 48 h.

For HTV/CF/clay composites, CF was first introduced into a toluene solution of HTV, and clay was then added after CF was well dispersed in the solution. The resulting solution was stirred under sonication and then dried in a vacuum oven at 60°C for 48 h. The HTV composites were cured under 19.4 atm using a hot press at 175°C for 10 min. Table I summarizes the composition of the HTV composites.

Assessment of thermal properties

TGA were performed to assess the thermal stability of the HTV composites using a TGA (TA Instruments, Q50, USA). The samples were heated at a heating rate of 20°C/min from 25 to 800°C under a dry nitrogen flow of 60 cm^3/min. Specimens of 15 mg weight were heated in an unconfined aluminum oxide cell, and the weight loss was monitored as a function of temperature.

The ablation properties were evaluated by measuring the insulation index. The back-face temperature record was measured with a thermocouple. The thermocouple was shielded with a mass of silicone rubber to allow accurate measurement of the back-face temperature, as shown in Scheme 1. The insulation index specimens were 70 mm × 70 mm × 6 mm in dimension. The oxy-acetylene torch tip was placed 2 cm away from the center of the front-face of the specimen. The insulation indexes were determined via the following equation (ASTM E 285[7]):

$$I_T = t_T/d$$

where I_T (s/m) is the insulation index at temperature T. t_T is the time elapsed for the back-face temperature to rise to 80, 130, 180, and 280°C, and d is the thickness of the specimen.

A new method was devised in this study to measure the ablation properties. A specimen with dimensions of 10 mm × 70 mm × 6 mm was hung clamped with 48.5 g of load. An oxy-acetylene flame was burst onto the center of the specimen and the time elapsed for the specimen to break off was measured. The volumetric flow rate of oxygen and acetylene was adjusted to be 1 : 1.2 (v/v).

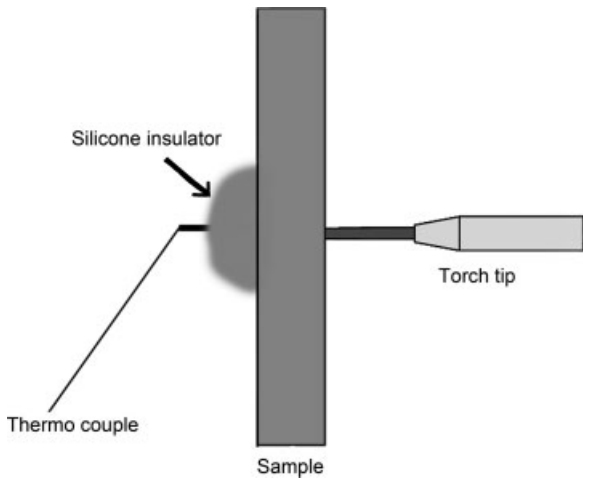

Scheme 1 Apparatus for the evaluation of the ablation properties.

Crosslinking density

The crosslinking density of the HTV composites was measured by measuring the degree of swelling in toluene. Square sheet samples with 2-mm thickness were cut into specimens of about 2 g weight, which were then soaked in toluene for 48 h at room temperature. The completely swelled specimens were wiped gently with a kitchen tissue to remove remaining solvent from the surface and their weight was subsequently measured.

Crosslinking density was calculated using the Flory-Huggins equation[8] as follows:

$$\nu_e = \frac{-N_A[\ln(1-V_R) + V_R + x_1 V_R^2]}{V_1(V_R^{1/3} - V_R/2)}$$

where ν_e is the crosslinking density per unit volume. N_A is the Avogadro's number. V_1 and V_R are the molar volume of the solvent and volume fraction of the polymer in the swelled specimen, respectively. The Flory-Huggins interaction parameter x_1 was set to be 0.45.[9]

Instruments

IR spectra of the HTV composites were recoded at a wave number range of 4000 cm^{-1}–400 cm^{-1} using Fourier Transform Infrared (FTIR, Perkin-Elmer, MA). X-ray diffraction patterns were obtained using a wide angle X-ray scattering (XRD, Rigaku DMAX 2500, Japan) with reflection geometry and CuKα radiation operated at 40 kV and 100 mA. Data were collected within a range of scattering angles (2θ) of 2–10°. The morphology of the composites was observed using a transmission electron microscopy

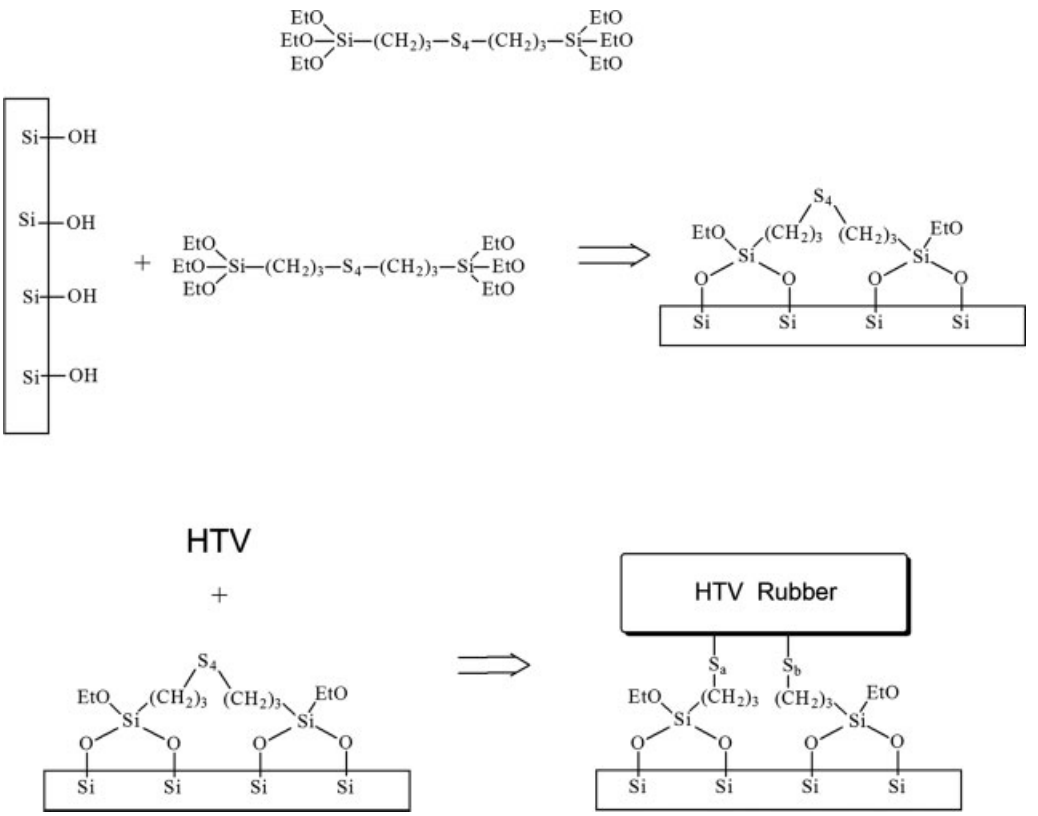

Scheme 2 Grafting of bis(3-triethoxysilylpropyl)tertra sulfide silane to clay surface and reaction of tertra sulfide groups with HTV.

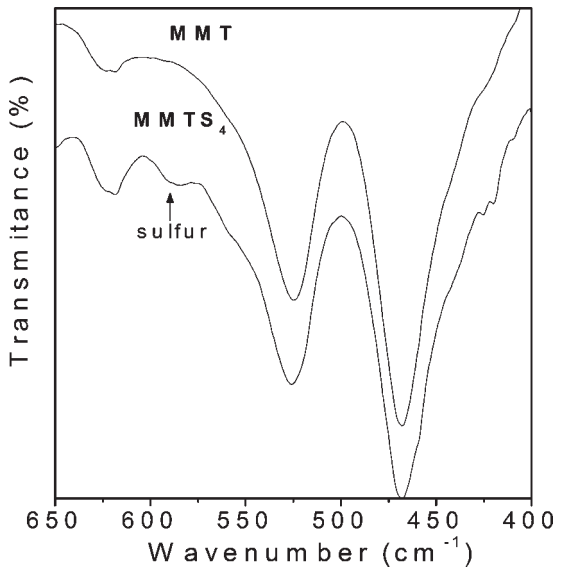

Figure 1 Fourier transform infrared spectra of the clays.

(TEM) (Philips CM200, The Netherlands) with an acceleration voltage of 120 kV. The dispersion of CF was examined with a scanning electron microscope (SEM, Hitach, S-4200, Japan).

RESULTS AND DISCUSSION

HTV/clay composites

Tetra sulfide (TS) groups were introduced to the surface of a commercially available clay, Cloisite®Na^+ (MMT), via reaction of the silanol groups of the clay with TEPTS to prepare $MMTS_4$, as shown in Scheme 2. Grafting of TEPTS to MMT was confirmed through FTIR observations and a TGA, as exhibited in Figures 1 and 2. Absorption peaks assignable to the C—H bonding vibration appeared at 2930 cm^{-1} and 2851 cm^{-1} and were observed in the FTIR spectrum of $MMTS_4$, whereas the same peak was absent

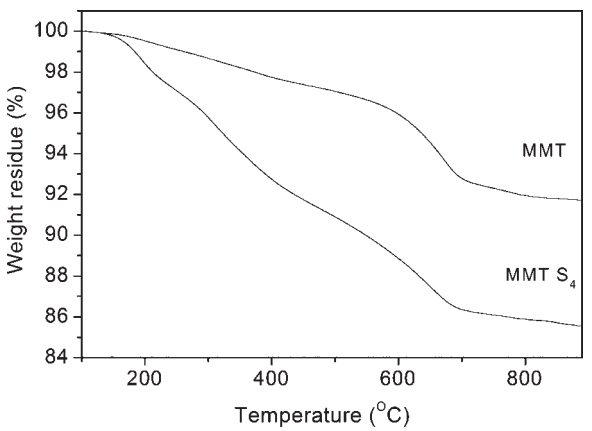

Figure 2 Thermogravimetric analysis results for the clays.

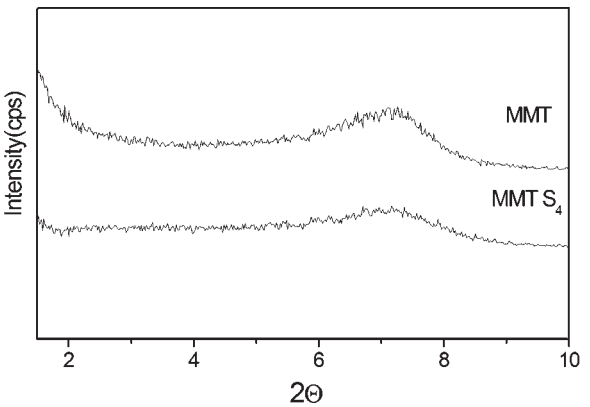

Figure 3 The X-ray diffraction the pattern of the clays.

in that of neat MMT. In addition, a peak appearing at 590 cm^{-1} for $MMTS_4$ corresponding to S—S—C stretching was observed, but neat MMT did not exhibit any peak at the same position.

TGA was performed for the two clays under a nitrogen atmosphere, as shown in Figure 2, after Soxhlet extraction with chloroform for a week to remove any unreacted TEPTS and complete drying in a vacuum oven. $MMTS_4$ and MMT lost 14.5 wt % and 9.3 wt % of their initial weight, respectively. The difference in the weight loss between the two clays is attributed to the additional weight loss because of the grafted TEPTS, thus confirming the successful grafting of TEPTS to MMT.

TS groups may react with the vinyl groups present in the HTV silicone rubber, as schematized in Scheme 2, to enhance the interaction between the clay and the silicone rubber.[10–12]

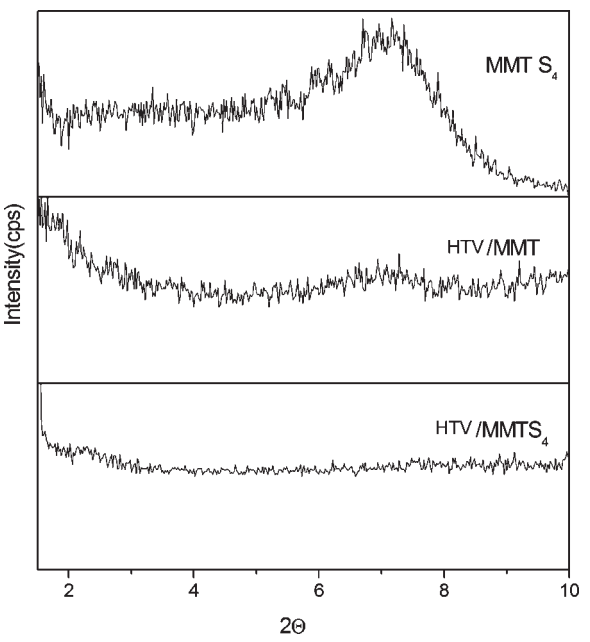

Figure 4 The X-ray diffraction pattern of the clays and the silicone rubber composites.

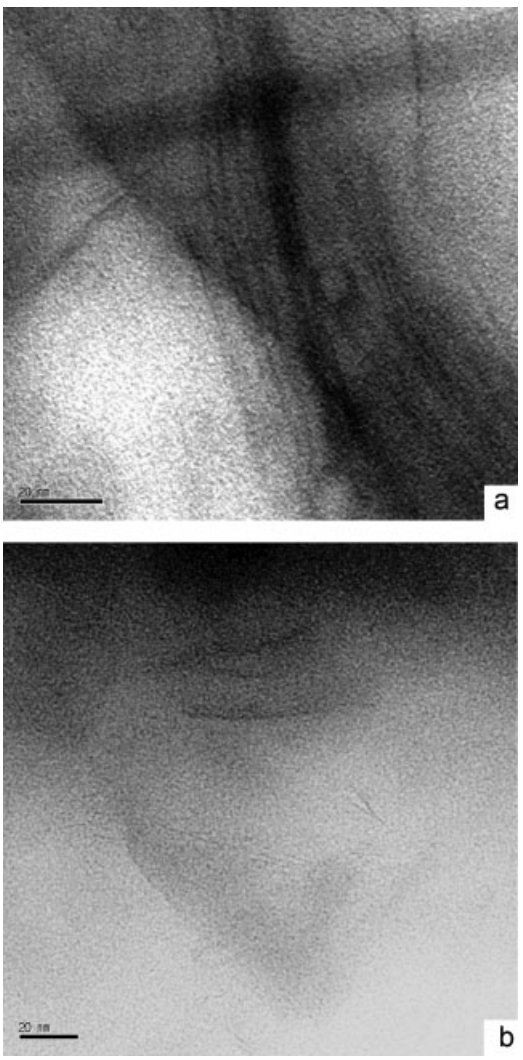

Figure 5 TEM photograph of the silicone rubber composites. (a: HTV/MMT, b: HTV/$MMTS_4$).

The amount of TEPTS grafted to MMT was estimated to be 0.2 mequiv/g from the TGA weight loss results according to the equation shown below.[13]

$$\text{Grafted amount (mequiv/g)} = (10^3 \times W_{200-600})/(100 - W_{200-600})/M$$

where M (g/mol) is the molecular weight of the silane molecules and $W_{200-600}$ is the weight loss observed between 200 and 600°C, which is supposed to be due to the silane compound degradation.

On the basis of the XRD results presented in Figure 3, the gallery basal spacing of MMT was measured to be 11.7 Å. The d_{001} peak of $MMTS_4$ also appeared at 2θ of about 7.2°, indicating that the interlayer spacing of MMT and $MMTS_4$ was similar in both cases. This is because the silanol groups are mostly concentrated on the edge of MMT rather than on its plain surface, and TEPTS molecules reacted for the most part on the edge of the clay layer. Herrera and his researchers as well as other groups reported similar findings.[13–16]

The two clays were compounded with HTV. The HTV/MMT composite exhibited a peak at the same 2θ position as the neat MMT, indicating that the crystalline stacked structure of the clay was preserved during compounding without discernible intercalation. In sharp contrast, the 2θ peak did not appear in the XRD of $MMTS_4$, as can be seen in Figure 4, indicating that some of the crystalline stacked

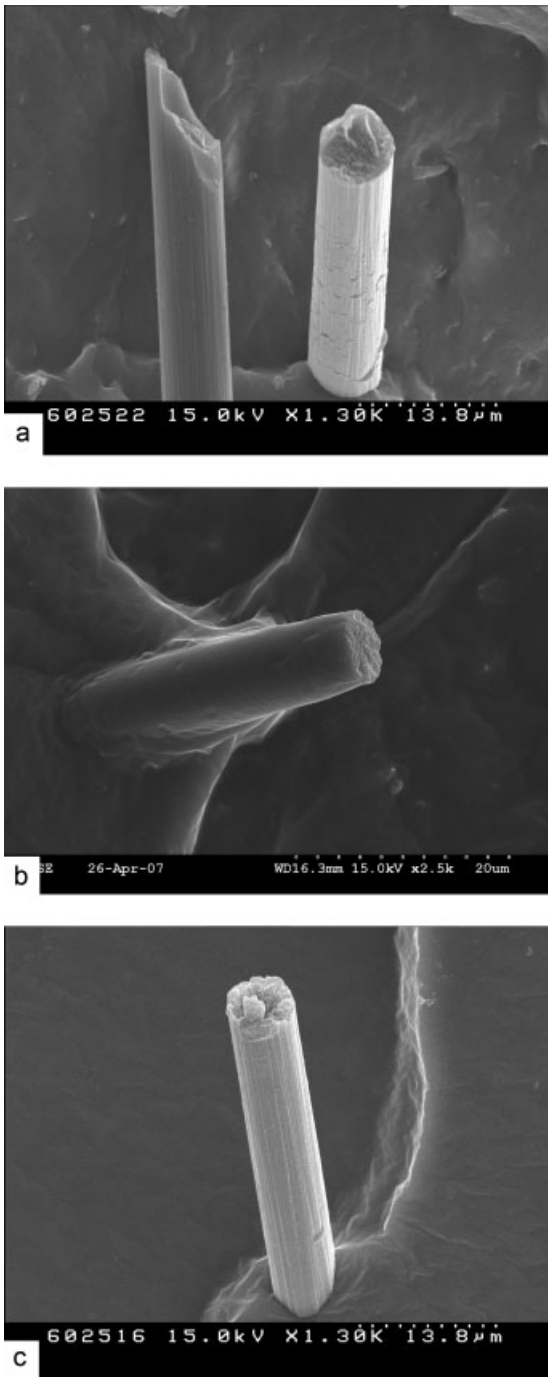

Figure 6 SEM image of the silicone rubber composites. (a: HTV/CF/MMT, b: HTV/CF/$MMTS_4$, and c: HTV/CF).

TABLE II
Specific Gravity and Crosslinking Density of the Silicone Rubber Composites

	HTV	HTV/MMT	HTV/CF/MMT	HTV/$MMTS_4$	HTV/CF/$MMTS_4$	HTV/CF
Specific gravity	0.965	1.090	1.078	1.014	1.1	0.956
Crosslinking density ($cm^{-3} \times 10^{20}$)	1.93	1.83	1.90	1.60	1.61	1.93

structure of the clay was destroyed, leading to some exfoliation.[17] The TEM image of the composites presented in Figure 5 confirms the above observations. It is surprising that, for the HTV/$MMTS_4$ composite, exfoliation took place to some extent even though intercalation was not observed in the HTV/MMT composite, because exfoliation is usually preceded by intercalation in most polymer/clay composites. It is plausible that the enhanced interaction between HTV and $MMTS_4$ made it possible to tear off the clay layers during the compounding in a layer-by-layer manner, similar to peeling off layers of an onion.

HTV/clay/carbon fiber composites

Carbon fiber (CF) was incorporated into the HTV/clay composites to prepare HTV/CF/MMT and HTV/CF/$MMTS_4$, respectively. CF usually exists in a bundle. Therefore, it needs to be dispersed in the matrix without being damaged. HTV was softly mixed with CF to break up the CF bundle without damaging the CF. It should be noted that, unlike HTV/CF and HTV/CF/MMT, CF in HTV/CF/$MMTS_4$ is evidently stained with the matrix HTV, as revealed in Figure 6. It is not clear at present why CF in HTV/CF/$MMTS_4$ was wetted more appreciably by the matrix HTV than the CF in the other composites. However, $MMTS_4$ may act as a compatiblizer between CF and HTV, if CF has some sites that are reactive toward TS groups, such as unsaturated double bonds.

Table II summarizes the specific gravity and the crosslinking density of HTV and HTV composites with the clays and CF. The former was obtained by using a picnometer, whereas the latter was measured from the degree of swelling in toluene. The interstice located at the interface between HTV and CF of the HTV/CF composite, as exhibited in the SEM image in Figure 6(c), is thought to be responsible for the slightly lower specific gravity of the HTV/CF composite compared with that of the neat HTV in spite of the higher density of CF relative to that of HTV. In the same manner, HTV/CF/MMT showed lower specific gravity than HTV/MMT. It is also interesting that the specific gravity of the HTV/CF/$MMTS_4$ composite was higher than that of all the other composites. The SEM image in Figure 6(b) supports this observation, in which the CF in the HTV/CF/$MMTS_4$ composite was well adhered to the matrix HTV, thus excluding the possibility of the presence of small voids between the interfaces.

The crosslinking density of the neat HTV is almost the same as that of either the HTV/MMT or the HTV/CF/MMT composites. However, the crosslinking density of the HTV/$MMTS_4$ composite is no higher than 83% that of the neat HTV. This can be rationalized by the assumption that some of the double bonds in HTV were exhausted because of the reaction with the TS groups of $MMTS_4$ and did not contribute to crosslinking.

Incorporation of CF into the composites has both adverse and favorable effects on the degree of swelling and hence on the apparent crosslinking density,

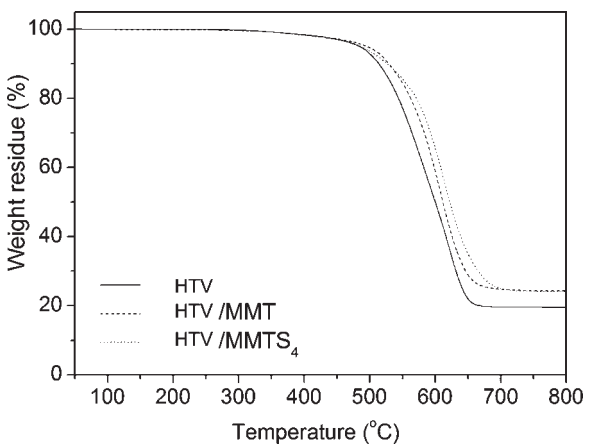

Figure 7 TGA results for HTV and its composites with the clays.

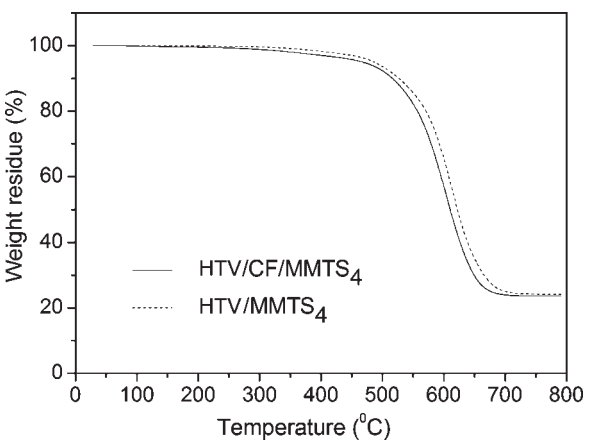

Figure 8 TGA results for the silicone rubber composites with the modified clay and carbon fiber.

TABLE III
Insulation Index of HTV and Its Composites

Bench mark temperature (°C)	HTV	HTV/2% MMT	HTV/5% MMT	HTV/2% $MMTS_4$	HTV/5% $MMTS_4$
80	6.7	9.0	11.2	11.2	11.3
130	14.0	14.7	20.2	14.6	19.1
180	21.3	21.9	34.2	21.7	29.9
280	30.7	40.8	51.1	40.7	57.1

because CF is not swelled by toluene and, at the same time, the interstice at the interface between CF and HTV may provide a site for toluene uptake. HTV/CF has lower density and higher crosslinking density compared with HTV. In the same context, HTV/CF/MMT possesses lower density and higher crosslinking density compared with HTV/MMT. Therefore, it can be said that the adverse effect of the CF incorporation on the toluene uptake was more significant than the favorable effect for those composites. In contrast, HTV/CF/$MMTS_4$ exhibits slightly higher crosslinking density as well as specific gravity than HTV/$MMTS_4$ does. This is because CF is well adhered to HTV in the HTV/CF/$MMTS_4$ composite, as can be observed in Figure 6(b), diminishing the interstice at the interface between CF and HTV.

Thermal properties of the composites

Figure 7 shows TGA diagrams for HTV and HTV composites with the clays. The onset temperature of thermal degradation of HTV rose due to the incorporation of MMT. Moreover, the HTV/$MMTS_4$ composite lost weight more slowly during the TGA than did the HTV/MMT composite, indicating that the composites with better dispersed clay layers are more thermally stable. The higher bonding energy of the *S*—C bond (699 kJ/mol) compared with that of the C—C bond (607 kJ/mol)[18] also would have contributed to the enhanced thermal stability. According to Figure 8, the HTV/CF/$MMTS_4$ composite began to lose weight at lower temperature than did the HTV/$MMTS_4$ composite. This is due, at least partially, to the increased thermal conductivity as a result of the incorporation of CF.

Ablation properties of the composites

The ablation properties of thermal insulators should be evaluated in an environment as harsh as that inside the combustion chamber of rocket motors. Ablation is defined as the heat and mass transfer process to dissipate the inflowing thermal energies by decomposing and burning down surface matters. Therefore, the ablation properties depend not only on the thermal stability of the thermal insulators but also on their energy dissipation efficiency. The mechanical properties of the char formed during combustion are also very important, because the char prevents direct contact of the flame with the motor case and delays heat transfer.

Because of its convenience of use, the oxy-acetylene torch test is frequently employed for the evaluation of the ablation properties. The oxy-acetylene torch flame is classified as carburizing flame, oxidizing flame, or neutral flame depending on the ratio of oxygen to acetylene. For a neutral flame, the temperature at a location 2 cm away from the torch tip reaches as high as 3200°C and decreases as the distance from the torch tip increases.[19]

The insulation index is used as an index for the ablation properties and is defined as the time elapsed to reach a certain temperature at the back side of a specimen with 6.4 mm thickness, after the oxy-acetylene flame bursts onto the front surface of the specimen. Table III summarizes the insulation index results.

The insulation index was raised by incorporation of MMT in the order of HTV < HTV/5% MMT ≤ HTV/5% $MMTS_4$, and the order was in line with that of the thermal stability determined from the TGA analysis. Vaia et al. also reported that ablation properties of nylon 6 composites were enhanced as a result of incorporation of clay.[20]

The char strength is very difficult to determine and the measurement of char thickness involves significant experimental error after the oxy-acetylene torch test.

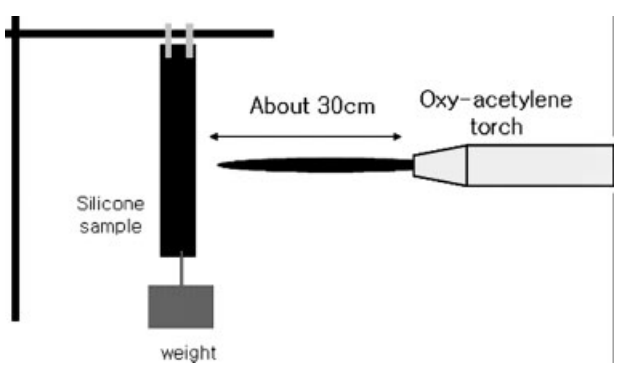

Scheme 3 Schematic illustration of the oxy-acetylene torch test for measurements of integrated ablation properties.

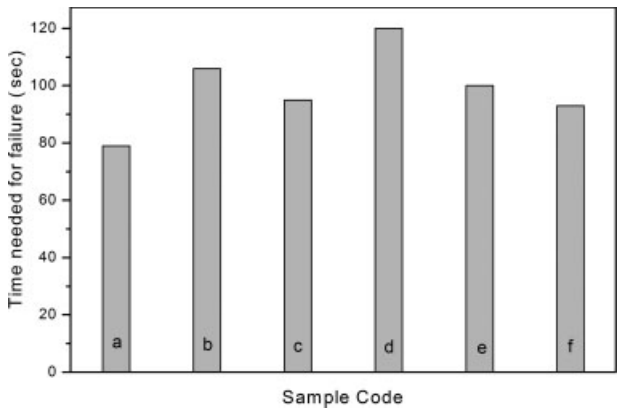

Figure 9 Time needed for failure of HTV and its composites during the oxy-acethylene torch test (a: HTV, b: HTV/MMT, c: HTV/$MMTS_4$, d: HTV/CF/MMT, e: HTV/CF/$MMTS_4$, and f: HTV/CF).

In this study, we devised a new method to determine the ablation properties, taking into consideration of the char strength as well as the rate of decomposition, as displayed in Scheme 3. The time elapsed for the specimen to break off was measured by oxy-acetylene flame. This time depends not only on the rate of decomposition but also on the mechanical strength of the char formed. Hence, we believe that this failure time can provide an index for the integrated ablation properties.

At least 10 specimens were tested to measure the failure time and the results were averaged as summarized in Figure 9. Incorporation of MMT into HTV raised the failure time significantly. Addition of CF to HTV/MMT composite further increased the failure time, because of the reinforcing effect of CF on the formed char. The increase of the failure time was more significant when CF was added to the HTV/MMT composite than to the neat HTV. The positive effect of CF incorporation on the improvement of the ablation properties has also been reported for other CF reinforced composites.[21–23]

Replacement of MMT with $MMTS_4$ reduced the failure time appreciably, as revealed in Figure 9. The time increased in the order of: HTV < HTV/CF≈HTV/$MMTS_4$ < HTV/CF/$MMTS_4$≈HTV/MMT < HTV/CF/MMT. This is contrary to expectations, because, according to the TGA diagram in Figure 8 and to the insulation index in Table III, the HTV/$MMTS_4$ composite is more thermally stable than the HTV/MMT composite. Although direct measurement of the mechanical strength of the char could feasibly clarify this issue, at present this cannot be easily achieved. The decreased degree of crosslinking of the composites with $MMTS_4$ compared with that of the composite with MMT may be unfavorable for the formation of mechanically strong char and could lead to early rupture of the HTV/$MMTS_4$ specimen.

Therefore, it can be concluded that the ablation properties assessed by different methods should be simultaneously taken into consideration and should be compared with the evaluation results obtained in an environment mimicking the combustion chamber of rocket motors.

References

1. Romanos, T. S.; Nacouzi, G. J.; Payne, G. A.; Norton, K. C. 31st AIAA/ASME/SAE/ASEE Joint Propulsion Conference, San Diego, CA, 1995; p. 3019.
2. Reynolds, R. A.; Nource, R. W.; Russell, G. W. 28th AIAA/ASME/SAE/ASEE Joint Propulsion Conference, Nashville, TN, 1992; p. 3056.
3. Guo, Y.; Liang, G.; Qiu, Z.; Liu, A. Mater Lett 2007, 61, 2406.
4. Pektas, I. J Appl Polym Sci 1998, 68, 1337.
5. Oyumi, Y. J Polym Sci Part A 1998, 36, 233.
6. Takasaki, H. F.; Annaka, M. O.; Sayama, H. O. U.S. Pat. 5,905,101 (1999).
7. ASTM. Annual Book of ASTM Standards; ASTM International: PA; Vol. 08.01, p E 285–E280.
8. Flory, P. J. Principles of Polymer Chemistry; Cornell University Press: New York, 1998.
9. Brandrup, J.; Immergut, E. H. Polymer Handbook, 3rd ed.; Wiley: New York, 1989.
10. Tian, M.; Liang, W.; Rao, G.; Zhang, L.; Guo, C. Compos Sci Technol 2005, 65, 1129.
11. Ismail, H.; Ishiaku, U. S.; Ishak, Z. A. M.; Freakley, P. K. Eur Polym Mater 1997, 33, 1.
12. Nasir, M.; Poh, B. T.; Nc, P. S. Eur Polym Mater 1989, 25, 267.
13. Herrera, N. N.; Letoffe, J. M.; Putaux, J. L.; David, L.; Lami, E. B. Langmuir 2004, 5, 1564.
14. Choi, S. S. Polym Test 2002, 21, 201.
15. López-Manchado, M. A.; Herrero, B.; Arroyo, M. Polym Int 2004, 53, 1766.
16. Ganter, M.; Gronski, W.; Reichert, P.; Mulhaupt, R. Rubber Chem Technol 2001, 74, 221.
17. Lebaron, P. C.; Pinnavaia, T. J Chem Mater 2001, 13, 3760.
18. Dean, J. A. Lange's Handbook of Chemistry, 5th ed.; McGraw-Hill: New York, 1999.
19. Messler, R. W., Jr. Principles of Welding: Processes, Physics, Chemistry, and Metallurgy; Wiley: New York, 1999.
20. Vaia, R. A.; Price, G.; Ruth, P. N.; Nguyen, H. T.; Lichtenhan, J. Appl Clay Sci 1999, 15, 67.
21. Tang, S.; Deng, J.; Liu, W; Yang, K. Carbon 2006, 44, 2877.
22. Patton, R. D.; Pittman, C. U., Jr.; Wang, L.; Hill, J. R.; Day, A. Compos Part A-Appl Sci Manuf 2002, 33, 243.
23. Tang, S.; Deng, J.; Wang, S.; Liu, W.; Yang, K. Mater Sci Eng A-Struct Mater 2007, 465, 1.